Hindawi
Geofluids
Volume 2022, Article ID 9159632, 12 pages
https://doi.org/10.1155/2022/9159632

Research Article

Analysis of the Internal Force and Deformation Characteristics of Double-Layer Lining Structure of Water Conveyance Tunnel

Yueyue Zhu,[1] **Cheng Liu**,[1,2] **Xiaotian Yin**,[1] **and Jingyu Zhang**[1]

[1]*School of Civil Engineering, Nanjing Forestry University, Nanjing, Jiangsu Province 210037, China*
[2]*Jiangsu Province Key Laboratory of Soil and Water Conservation and Ecological Restoration, Nanjing 210037, China*

Correspondence should be addressed to Cheng Liu; lcheng83@163.com

Received 15 February 2022; Revised 13 March 2022; Accepted 11 April 2022; Published 30 April 2022

Academic Editor: Yue Niu

Shield double-layer lining structure is used to bear large internal water pressure in water conveyance tunnel engineering, but the mechanism of joint stress of structure and force transmission between linings is still unclear. In this paper, a stress calculation model of the double-layer lining structure of shield water conveyance tunnel considering the influence of transition layer between the inner lining and the outer lining is presented. By analyzing the inner lining and outer lining separately, the calculation formulas of radial displacement and circumferential stress are obtained. Then, according to the deformation coordination condition, the relationship between the inner and outer lining radial displacements is established. Thus, the magnitude of the unknown interaction force among the structures is calculated. Finally, through the stress analysis of the lining structure, the axial force, shear force, and bending moment acted on the structure are obtained. By comparing finite element calculation results with analytical calculation results, the rationality of analytical solutions is verified. Based on the proposed analytical method, the influence of inner lining thickness and material parameters of transition layer on the internal force and deformation of lining structure is analyzed. The results show that with the increase of the thickness of the inner lining, the axial force and bending moment increase, while the internal pressure shared by the outer lining decreases. The larger the elastic modulus of the transition material, the smaller the difference between the internal force and deformation of the inner and outer linings.

1. Introduction

Nowadays, the double-layer lining structure of shield tunnels is increasingly used in submarine railway tunnels [1, 2], urban large-scale water pipelines [3, 4], and pressurized water conveyance tunnels [5, 6]. Because of its remarkable advantages in waterproofing, durability, and bearing capacity, double-layer lining has become the preferred structural type in the pressurized water conveyance tunnel project. This structure has been used in many projects already built and under construction, such as the Lanzhou Water Source Project [7], South-to-North Water Transfer Tunnel Crossing Yellow River Project [8, 9], and Pearl River Delta Water Resources Allocation Project [10]. Among them, the South-to-North Water Diversion Project crossing the Yellow River tunnel has a total length of about 19.3 km, a buried depth of 23~35 m, a shield outer diameter of 8.7 m, and a designed internal water pressure of 0.517 MPa. The lining is of double-layer structure, the outer lining is assembled by staggered joints of 7 reinforced concrete precast segments, and the inner lining is of 450 mm thick concrete structure. The double-layer lining of the shield tunnel is a kind of combined lining composed of assembled segments of shield and secondary lining. The joint stress analysis and structural design calculation of this structure are still in the exploratory stage, and there is a lack of an effective unified calculation method [11, 12].

Combined with the construction practice of shield tunnels [13–15], many scholars have made relevant research on double-layer lining structures from three aspects: model test, numerical analysis, and theoretical analysis. The model test is an important way to study the problem. Based on the similar model test of the Shiziyang Tunnel, Wang et al. [1] studied the influence of the joint type of double-layer lining

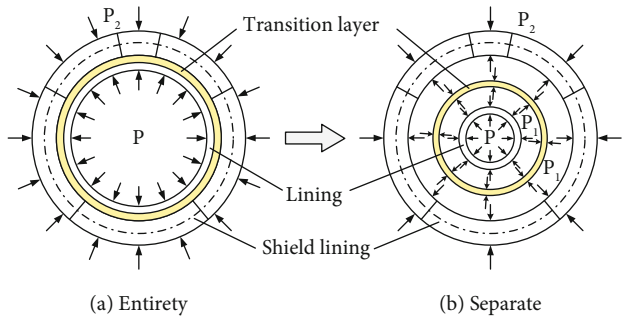

Figure 1: Mechanical analysis model of composite double-layer lining.

structure of shield tunnel on the mechanical behavior and failure characteristics of lining structure, which can guide the selection and design of the structure. Jin et al. [16] studied the mechanical behavior of two kinds of segment joints of double-layer lining through a series of full-scale laboratory tests. In the face of a complex environment and unclear force, numerical analysis can play a great auxiliary role in structural analysis and design [17–19]. Yan et al. [20] numerically analyzed the mechanical properties of a large-diameter double-layer lining tunnel under fire and high temperature, and the results showed that the tunnel structure had obvious expansion deformation and stress changes under high temperature. Simanjuntak et al. [6] determined the position where cracks are most likely to occur in the secondary lining through finite element model analysis, which is helpful to take measures to improve the sealing and stability of the tunnel. For the convenience of engineering design and theoretical analysis, the theoretical calculation of double-layer lining structure has important research value. Chen et al. [21] put forward the analytical solution of the joint lining of shield tunnel reinforced by secondary lining based on the curved Euler beam theory, which can effectively solve the internal force and deformation under various complex conditions. Naggar et al. [22] put forward an analytical method to calculate the in-plane moment and thrust of composite lining under earthquake, which is limited to the analysis of circular tunnels with complete or solid structures. Do et al. [23] derived the closed solution of the structure in the form of an integral equation for the deep circular tunnel supported by double-layer lining. Murakami and Koizumi [24] put forward an analytical model of double-layer lining structure based on the test results and applied it to the actual design of the shield tunnel. However, the above research on double-layer lining did not involve the influence of internal water pressure.

The stress and deformation of the tunnel itself are complicated [25–34], and the lining structure of the water conveyance tunnel not only bears external water and soil loads but also is subjected to greater internal water pressure. Guo et al. [4] conducted a model test on the drainage shield tunnel and studied the mechanical behavior and failure forms of the lining structure under the combined action of external water and soil load and internal water pressure. Li et al. [35] derived the stress distribution of composite lining based on the elastic theory, considering the influence of internal water pressure and surrounding rock on the composite lining. In this study, the lining and surrounding rock are analyzed as a whole, without considering the form of force transmission between double-layer linings. The coordinated deformation and stress mechanism of double-layer lining structure under internal and external pressure is complicated, especially the form and magnitude of the force on the contact surfaces of each structure are difficult to determine.

In this paper, a stress calculation model of the double-layer lining structure of shield water conveyance tunnel considering the influence of transition layer will be given. By analyzing the stress of each structure separately, considering the radial compression deformation of lining material, the magnitude of force transmission on the contact surface of each structure is obtained. The stress and deformation of the lining structure are obtained by elastic theory, and the bending moment of the structure is obtained by integrating the circumferential stress of the lining. Then, based on the rationality of the analytical solution verified by the results of finite element analysis, the influence of lining thickness and transition layer material parameters on the internal force and deformation of lining structure is analyzed by the analytical method given in this paper.

2. Analysis Model and Method

In this section, by simplifying the stress of the lining structure of the water conveyance tunnel, a new stress analysis model of composite double-layer lining is put forward. By analyzing the stress of inner and outer linings independently, the calculation formulas of radial displacement and circumferential stress are given. Then, according to the deformation coordination condition, the relationship between the radial displacement of inner and outer linings is established. On this basis, the unknown force P_1 on the lining structure can be calculated. Finally, according to the stress model, the stress of the lining structure is analyzed, and then, the axial force, shear force, and bending moment produced on the structure are obtained.

2.1. Establish Analysis Model. The lining structure of the water conveyance tunnel in the project is in a complex stress environment, with a combination of the gravity and pressure of water inside, the gravity of surrounding soil and groundwater outside, the self-weight of each structure, and the external resistance caused by structural deformation.

For simple calculation, the pressure on the outer surface of the lining is taken as the uniform pressure equal to the minimum water and soil pressure. Moreover, the influences of lining structure, water deadweight, and external resistance are not considered. Under the action of uniformly distributed internal water pressure and uniformly distributed external water and soil load, the stress calculation model of double-layer lining structure of shield water conveyance tunnel considering the influence of transition layer is established, as shown in Figure 1.

A layer of transition material is filled between the outer assembled segment and the inner lining. It is considered that

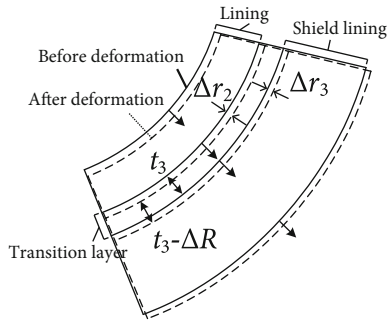

Figure 2: Radial displacement of lining structure.

the transition layer only transmits radial force and neglects its consumption of force. It is known that the uniform internal pressure is P, and the uniform external pressure is P_2. If the reaction force of the transition layer material to the inner lining is P_1, the pressure transmitted from the transition layer to the outer lining is $P_1' = P_1$.

To calculate the internal force and deformation of the lining structure, it is necessary to calculate the magnitude of the unknown force. The value of unknown force P_1 is solved by establishing the deformation coordination relationship between inner and outer linings and combining the displacement calculation formula obtained by independent analysis of inner and outer linings.

(1) Deformation coordination relation

Under the action of uniform pressure inside and outside, the lining structure will produce certain compression deformation, which, in turn, leads to the change of inner and outer lining radius. The deformation is shown in Figure 2, and the deformation coordination relation is

$$\Delta R = \Delta r_2 - \Delta r_3, \tag{1}$$

where ΔR is the compression deformation of transition material between two linings. Δr_2 and Δr_3 are the increase of inner radius and outer radius, respectively.

(2) Stress analysis of inner lining

The inner lining is subjected to the internal uniform water pressure P and the uniform reaction force P_1 exerted by the transition layer. The independent analysis model is shown in Figure 3(a). According to the theory of thick-walled cylinder in elasticity, the radius increment Δr and circumferential tensile stress σ_φ at any position of the inner lining can be obtained, and the calculation formula is as follows:

$$\begin{aligned}\Delta r = &\left(\frac{1-\mu}{E}\frac{r_1^2\rho}{r_2^2-r_1^2} + \frac{1+\mu}{E\rho}\frac{r_1^2r_2^2}{r_2^2-r_1^2}\right)P \\ &- \left(\frac{1-\mu}{E}\frac{r_2^2\rho}{r_2^2-r_1^2} + \frac{1+\mu}{E\rho}\frac{r_1^2r_2^2}{r_2^2-r_1^2}\right)P_1,\end{aligned} \tag{2}$$

$$\sigma_\varphi = \frac{r_1^2P - r_2^2P_1}{r_2^2-r_1^2} - \frac{r_1^2r_2^2}{r_2^2-r_1^2}\frac{P_1-P}{\rho^2}, \tag{3}$$

where r_1 and r_2 are the inner and outer radii of the ring, respectively. ρ is the polar diameter at the calculated position. μ is Poisson's ratio. E is the elastic modulus of the material.

(3) Stress analysis of outer lining

The external shield lining ring is affected by the uniformly distributed internal pressure P_1 transmitted by the transition layer and the uniformly distributed external water and soil pressure P_2. The independent analysis model is shown in Figure 3(b). According to the thick-walled cylinder theory, the radius increment Δr and circumferential stress σ_φ at any position of the outer lining can be obtained. The calculation formula is as follows:

$$\begin{aligned}\Delta r = &\left(\frac{1-\mu}{E}\frac{r_3^2\rho}{r_4^2-r_3^2} + \frac{1+\mu}{E\rho}\frac{r_3^2r_4^2}{r_4^2-r_3^2}\right)P_1 \\ &- \left(\frac{1-\mu}{E}\frac{r_4^2\rho}{r_4^2-r_3^2} + \frac{1+\mu}{E\rho}\frac{r_3^2r_4^2}{r_4^2-r_3^2}\right)P_2,\end{aligned} \tag{4}$$

$$\sigma_\varphi = \frac{r_3^2P_1 - r_4^2P_2}{r_4^2-r_3^2} - \frac{r_3^2r_4^2}{r_4^2-r_3^2}\frac{P_2-P_1}{\rho^2}, \tag{5}$$

in which r_3 and r_4 are the inner and outer radii of the ring.

2.2. Unknown Force P_1 Solution. The stress equivalent model of composite double-layer lining is established as shown in Figure 1. On this basis, the inner and outer linings are separately analyzed in Section 2.1, and their respective radial displacement and circumferential stress calculation expressions are obtained. In the following, through the deformation coordination condition, the formulas for calculating the increase of the outer radius of the inner lining and the inner radius of the outer lining will be simultaneously established. Further, the reaction force P_1 of the transition layer material to the inner lining is obtained.

From the above, the expressions for calculating the increase of inner radius and outer radius can be obtained, respectively:

$$\begin{aligned}\Delta r_2 = &\left(\frac{1-\mu_1}{E_1}\frac{r_1^2r_2}{r_2^2-r_1^2} + \frac{1+\mu_1}{E_1r_2}\frac{r_1^2r_2^2}{r_2^2-r_1^2}\right)\bullet P \\ &- \left(\frac{1-\mu_1}{E_1}\frac{r_2^3}{r_2^2-r_1^2} + \frac{1+\mu_1}{E_1r_2}\frac{r_1^2r_2^2}{r_2^2-r_1^2}\right)\bullet P_1 \\ = &\, k_1\bullet P - k_2\bullet P_1,\end{aligned} \tag{6}$$

$$\begin{aligned}\Delta r_3 = &\left(\frac{1-\mu_2}{E_2}\frac{r_3^3}{r_4^2-r_3^2} + \frac{1+\mu_2}{E_2r_3}\frac{r_3^2r_4^2}{r_4^2-r_3^2}\right)\bullet P_1 \\ &- \left(\frac{1-\mu_2}{E_2}\frac{r_4^2r_3}{r_4^2-r_3^2} + \frac{1+\mu_2}{E_2r_3}\frac{r_3^2r_4^2}{r_4^2-r_3^2}\right)\bullet P_2 \\ = &\, k_3\bullet P_1 - k_4\bullet P_2,\end{aligned} \tag{7}$$

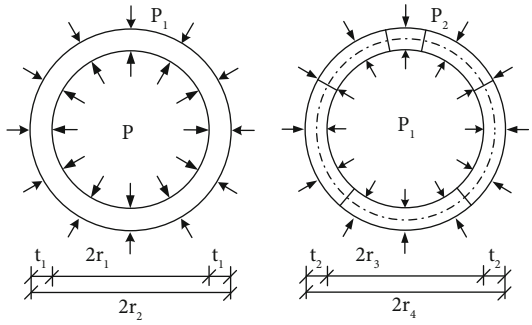

(a) Inner lining (b) Outer lining

Figure 3: Analysis model of inner and outer linings.

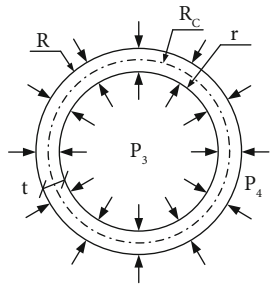

Figure 4: Calculation model of lining ring under uniform internal and external pressure.

where E_1 and E_2 are the elastic moduli of the inner lining and the outer lining, respectively. μ_1 and μ_2 are Poisson's ratios of the inner lining and outer lining, respectively.

According to the stress calculation model established in Section 2.1, the pressure on the inner and outer surfaces of the transition layer is P_1. According to Hooke's law, the formula for calculating the compressive deformation ΔR of the transition material between two linings is as follows:

$$\Delta R = \frac{P_1 \bullet t_3}{E_3} = k_5 \bullet P_1, \tag{8}$$

where E_3 is the elastic modulus of transition material. t_3 is the thickness of the transition layer.

By substituting Equations (6), (7), and (8) into Equation (1), the calculation expression of uniform pressure P_1 on the outer surface of the inner lining and the inner surface of the outer lining can be obtained as follows:

$$P_1 = \frac{k_1 \bullet P + k_4 \bullet P_2}{k_2 + k_3 + k_5}. \tag{9}$$

To sum up, the calculation formula of the unknown force P_1 has been obtained. And the corresponding parameter values can be obtained only by substituting them into the calculation expressions of inner and outer lining radius increment Δr and circumferential stress σ_φ.

2.3. Internal Force Calculation of Lining. The internal force analysis of the lining structure is an important step in the process of tunnel design. The calculation of bending moment in the existing guidelines for shield tunnel design mostly takes the structure as the analysis object based on the analysis method of structural mechanics. Based on the analysis model in Figure 1, the calculation expression of bending moment proposed in this section is obtained by integrating the calculation formula of lining circumferential stress given by elasticity, instead of taking the structure as the analysis object.

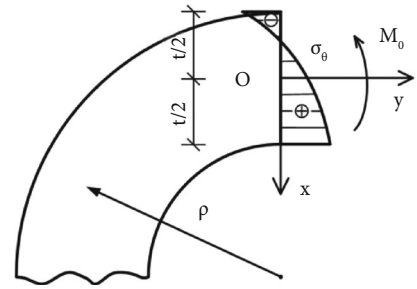

Figure 5: The angle θ_0 corresponds to the circumferential stress distribution at the radial thickness.

The stress model of the lining ring under uniform internal pressure and uniform external pressure is shown in Figure 4.

In the drawing, r, R, and R_C are the inner radius, outer radius, and centroid radius of the lining ring, respectively. t is the thickness of the lining ring. P_3 and P_4 are the uniformly distributed pressures acting on the inner and outer surfaces of the lining, respectively. According to the model in Figure 4, the axial force, shear force, and bending moment on the lining ring are, respectively, solved in the following:

(1) Axial force

Taking half of the lining ring structure for stress analysis, the calculation expression of axial force N can be derived from the relevant knowledge in material mechanics, as follows:

$$2N = \int_0^\pi (P_3 - P_4) \sin\theta \bullet R_c d\theta = 2(P_3 - P_4) \bullet R_c. \tag{10}$$

Get:

$$N = (P_3 - P_4) \bullet R_c. \tag{11}$$

The model is symmetrical about any straight line passing through the diameter, so the inner axial force of the lining is $(P_3 - P_4) \bullet R_c$ (negative tension and positive compression) everywhere.

(2) Shear force

The lining is a ring with equal thickness, and the internal and external pressures are evenly distributed. Therefore, the adjacent planes of the lining will not have relative displacement or dislocation in the radial direction, and there is no trend of this movement.

Table 1: Material parameter table for model calculation.

Material	E (kPa)	γ (kN/m^3)	μ
Outer lining	3.34e6	25	0.25
Transition layer (rubber)	7.8e3	15	0
Inner lining	1e7	25	0.24

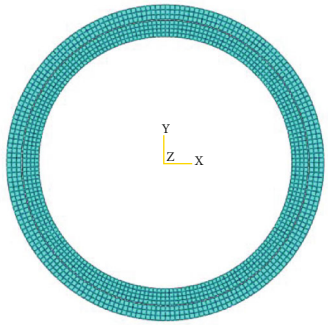

Figure 6: Finite element calculation model.

Therefore, the radial shear force in the lining is assumed to be zero everywhere.

(3) Bending moment

① According to the theory of thick-walled cylinder, the calculation expression of circumferential stress at any point on the lining under uniform internal and external pressure is

$$\sigma_\theta = \frac{r^2P_3 - R^2P_4}{R^2 - r^2} + \frac{r^2R^2}{R^2 - r^2}\frac{P_3 - P_4}{\rho^2}, \tag{12}$$

where σ_θ is the circumferential stress at $M(\rho, \theta)$ point in polar coordinates corresponding to the lining. ρ is the polar diameter at the calculated position.

② Since the lining shape and external force are symmetrical, the cross-section corresponding to the θ_0 angle can be arbitrarily selected for stress analysis. According to σ_θ expression, circumferential stress distribution in cross-section can be roughly drawn, as shown in Figure 5.

The lining thickness is t, taking the centroid of the cross-section as the origin. A Cartesian coordinate system as shown in Figure 5 is established, which is $\rho = r + (t/2) - x$. Substituting $g = r + (t/2)$, $m = (r^2P_3 - R^2P_4)/(R^2 - r^2)$, and $n = (r^2R^2\bullet(P_3 - P_4))/(R^2 - r^2)$ into the solution formula of σ_θ, the expression of σ_θ corresponding to the coordinate system in Figure 5 can be obtained as follows:

$$\sigma_\theta = m + n\bullet\frac{1}{(g - x)^2}. \tag{13}$$

③ Calculate the bending moment relative to the centroid o point by integration:

$$M_O = \int_{-t/2}^{t/2}\sigma_\theta\bullet x\bullet dx = \int_{-t/2}^{t/2}\left[m + n\bullet\frac{1}{(g - x)^2}\right]\bullet x dx. \tag{14}$$

Substitute $t = R - r$, $m = (r^2P_3 - R^2P_4)/(R^2 - r^2)$, $n = (r^2R^2\bullet(P_3 - P_4))/(R^2 - r^2)$, and $g = r + (t/2)$ to get

$$M_O = \left(\frac{1}{2}r\bullet R + \frac{r^2R^2}{R^2 - r^2}\bullet\ln\frac{r}{R}\right)\bullet(P_3 - P_4). \tag{15}$$

To sum up, the bending moment in the lining is everywhere: $M = ((1/2)r\bullet R + (r^2R^2/(R^2 - r^2))\bullet\ln(r/R))\bullet(P_3 - P_4)$, and the direction is from inside to outside (same as the direction in Figure 5).

3. Finite Element Verification and Analysis

To verify the correctness of the calculation model and method in this paper, numerical analysis and analytical solution are used to calculate the deformation and stress values of the lining structure of the Yellow River Tunnel of the South-to-North Water Transfer Project. At the same time, the influence of the thickness of the transition layer is analyzed, and the difference between the two methods is compared.

3.1. Water Transfer Project of South-to-North Water Transfer Tunnel Crossing Yellow River. The designed internal water pressure of the South-to-North Water Diversion Tunnel across the Yellow River is 0.517 MPa. The minimum buried depth of the tunnel is 23 m, the stratum it mainly crosses is a sand layer, and the elastic modulus is 20 MPa. Considering that the Yellow River is wandering, the flow rate decreases obviously in the dry season. The external water and soil load are calculated on the ground according to the water level, and the minimum external water and soil pressure is 0.3 MPa [10]. The outer diameter of the shield is 8.7 m, the outer lining is composed of precast segments with a thickness of 400 mm, and the inner lining is a concrete structure with a thickness of 450 mm.

According to the design data of the project, the finite element analysis software is used to establish the water conveyance tunnel model, and the tunnel parameters required for simulation are the same as the analytical solution, as shown in Table 1. The transition layer is in a closed space, and its lateral deformation is not considered according to the assumption of the analytical model, so Poisson's ratio is set as 0. The outer lining is a shield assembled segment. Considering the weakening effect of the joint part, its equivalent elastic modulus is 3.34 GPa for calculation.

The finite element model is applied with 0.517 MPa uniformly distributed internal water pressure and 0.3 MPa uniformly distributed external water and soil pressure. Tie connection is adopted among all components. The horizontal displacement of the top and bottom cross-sections of the structure and the vertical displacement of the leftmost and rightmost cross-sections of the structure are constrained.

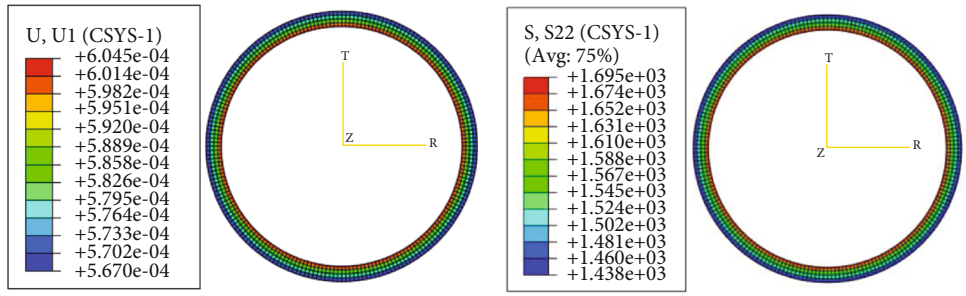

(a) Radial deformation of inner lining (b) Circumferential stress of inner lining

Figure 7: Radial deformation and circumferential stress of inner lining.

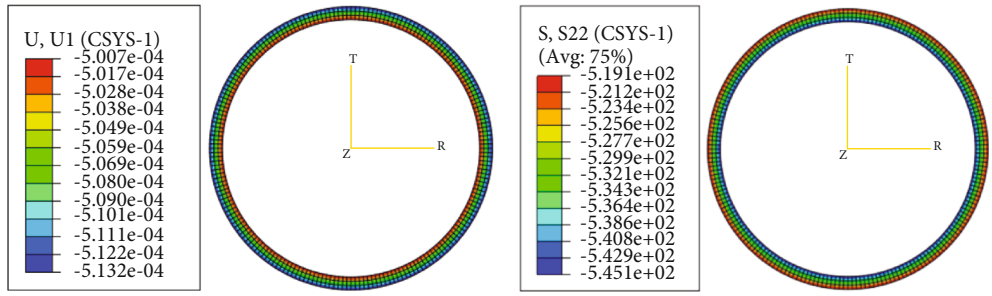

(a) Radial deformation of outer lining (b) Circumferential stress of outer lining

Figure 8: Radial deformation and circumferential stress of outer lining.

Table 2: Numerical analysis results.

Location	Δr (mm)	σ_φ (MPa)
Inner radius of inner lining	0.605	1.70
Inner radius of outer lining	-0.501	-0.545

Table 3: Analytical solution results.

Location	Δr (mm)	σ_φ (MPa)	N (kN)	Q (kN)	M (kN·m)
Inner radius of inner lining	0.619	1.66	870	0	3.96
Inner radius of outer lining	-0.498	-0.492	-76.6	0	-0.246

All the components adopt the CPE4I plane strain four-node nonconforming element. The outer radius of the shield segment is 4.35 m, and the inner radius is 3.95 m. The outer radius of the transition layer is 3.95 m, and the inner radius is 3.92 m. The inner lining has an outer radius of 3.92 m and an inner radius of 3.47 m. The finite element model and some calculation results are shown in Figure 6:

As shown in Figure 7, under the action of uniformly distributed internal water pressure and the reaction force of the transition layer, the radial deformation and circumferential stress of the inner lining gradually decrease from inside to outside. As shown in Figure 8, under the action of external water and soil load and the reaction force of the transition layer, the outer lining is deformed inward. At this time, the lining is subjected to compressive stress in the circumferential direction, and the compressive stress value gradually increases from the outside to the inside.

The finite element calculation result data is summarized by the finite element result diagram, as shown in Table 2. The corresponding calculation results are shown in Table 3.

It can be seen from the data in Tables 2 and 3 that the numerical simulation results are basically consistent with the calculated results. Compared with numerical results, the maximum error of radius increment is about 2%, and the maximum error of circumferential stress is about 10%, all of which are in a small range. Therefore, the rationality of the calculation model and method in this paper can be verified.

The main reasons for the errors between the analytical solution and the numerical results are as follows: (1) In the analytical solution, the dissipation of the force when the transition layer material transfers the radial stress is ignored, and it is considered that all the forces transferred from the inner lining are transferred to the outer lining. (2) Poisson's ratio of transition layer material is set to 0 in the numerical analysis model, which is inconsistent with the actual situation. Therefore, there are some errors in the deformation and stress results of inner and outer linings, and these aspects need to be further improved.

3.2. Analysis of Influence of Transition Layer Thickness. Setting the transition layer between the inner lining and the outer lining can not only play the role of drainage and water

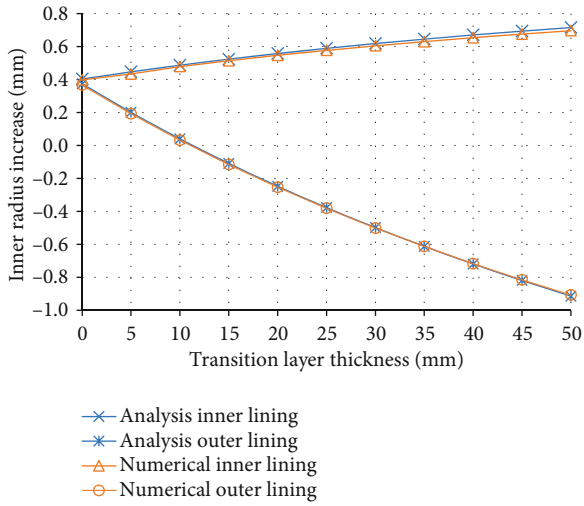

Figure 9: Increase of inner radius of inner and outer linings with different thickness of transition layer.

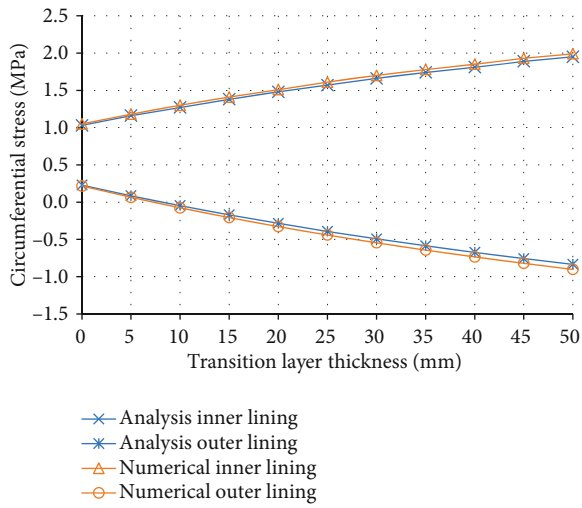

Figure 10: Circumferential stress at inner radius of inner and outer linings with different thickness of transition layer.

Table 4: Calculation parameter table.

Material	E (kPa)	μ	r (m)	R (m)
Outer lining	3.34e6	0.25	3.95	4.35
Transition layer (rubber)	7.8e3	0	3.93	3.95
Inner lining	1e7	0.24	x	3.93

insulation but also establish an effective connection between the inner lining and the outer lining. The stress and deformation of the double-layer lining structure of the water conveyance tunnel can be optimized by setting the parameters of the transition layer reasonably. The influence of the thickness of the transition layer on the lining structure is compared and analyzed by finite element analysis and analytical solution.

Based on the model in Section 3.1, the structural materials, outer lining size, and inner lining thickness are kept unchanged, and the thickness of the transition layer material is modified. Then, the inner radius increase and circumferential stress of inner and outer linings with the thickness of 0, 5, 10, 15, 20, 25, 30, 35, 40, 45, and 50 mm are calculated, respectively. The results of numerical analysis and analytical solution are shown in Figures 9 and 10.

It can be seen from the calculation results that the radial deformation and circumferential stress of inner radius of inner and outer linings obtained by numerical calculation and analytical solution of changing the thickness of transition layer are basically consistent, and the error is very small. Furthermore, the correctness of the analytical solution proposed in this paper is verified.

It can be seen from the line chart that the radial displacement and circumferential stress of the inner and outer linings change with the thickness of the transition layer. With the reduction of the thickness of the transition layer, the radial deformation and circumferential stress of the inner lining decrease, while the radial deformation and circumferential stress of the outer lining increase. The inner radius increase and the circumferential stress of inner and outer linings are gradually consistent. When the thickness is 0, the displacement values of the inner radius of two linings are approximately equal. When the thickness of the transition layer is about 10 mm, the inner radius increase of the outer lining and the circumferential stress are in the critical position of changing from positive to negative.

4. Influencing Factors of Internal Force and Deformation of Lining Structure

Compared with the setting of the inner lining and transition layer, the type of segment assembled by the outer lining is relatively fixed in a double-layer shield water conveyance tunnel, so it is not taken as the analysis object here. Based on the Yellow River Tunnel Project of the South-to-North Water Transfer Project, the influence of inner lining thickness and transition layer material parameters on the internal force and deformation of the lining structure is analyzed by the analytical solution given in this paper.

4.1. Influence of Inner Lining Thickness on Internal Force and Deformation of Structure. The thickness of the inner lining has an impact on the deformation and stress of the whole structure. To make the stress distribution and deformation control among the structures more reasonable, the influence of the thickness of the inner lining on the internal force and deformation of the double-layer lining structure is studied according to the model parameters in Table 4.

The inner radius of the inner lining is 3.73, 3.68, 3.63, 3.58, 3.53, 3.48, and 3.43 m, respectively. The lining structure bears 0.517 MPa internal uniform water pressure and 0.3 MPa external uniform water and soil pressure. According to the calculation method provided in this paper, the radius increment and circumferential stress at the inner radius of the inner and outer linings, as well as their respective axial

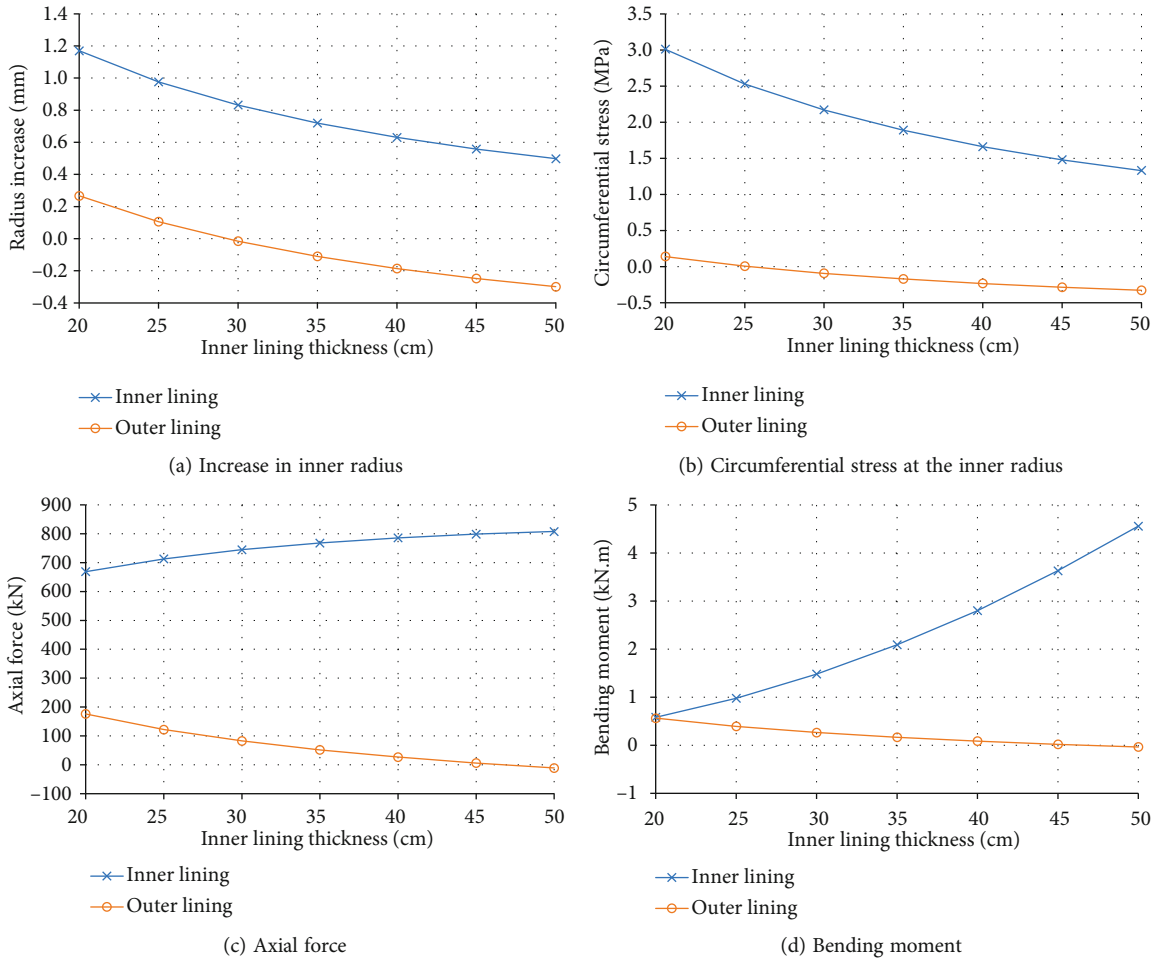

Figure 11: Influence of inner lining thickness on internal force and deformation of lining structure.

Table 5: Calculation parameter table.

Material	E (kPa)	μ	r (m)	R (m)	t (m)
Outer lining	3.34*e*6	0.25	3.95	4.35	0.4
Transition layer	y	0	3.93	3.95	0.02
Inner lining	1*e*7	0.24	3.48	3.93	0.45

forces and bending moments, are calculated, respectively, as shown in Figure 11.

It can be seen from Figure 11(a) that with the increase of inner lining thickness, the increasing amount of inner radius of the inner lining and outer lining decreases continuously, and the decreasing rate gradually slows down. When the thickness of the inner lining is 30 cm, the inner radius increase of the outer lining is approximately zero, reaching the critical value that the outer lining changes from outward deformation to inward deformation. With increasing thickness of the inner lining, the internal water pressure transmitted to the outer lining reduces, and it is more obvious that the inner and outer linings bear the internal and external pressure alone. Therefore, setting the thickness of the inner lining reasonably can optimize the radial deformation of the inner and outer linings and the external force they bear.

It can be seen from Figure 11(b) that with the increase of the thickness of the inner lining, the circumferential stress at the inner radius of the inner and outer linings decreases continuously. The circumferential stress at the inner radius of the inner lining decreases greatly, while the circumferential stress at the inner radius of the outer lining changes little. When the thickness of the inner lining is 26 cm, the circumferential stress at the inner radius of the outer lining is almost zero. With the thickness of the inner lining increasing, the inner radius of the outer lining is compressed and the pressure value increases continuously. The circumferential stress at the inner radius of the inner lining is much larger than that of the outer lining, so the inner lining should adopt the integral structure to avoid the large gap at the joint caused by excessive circumferential stress.

It can be seen from Figure 11(c) that with the increase of the thickness of the inner lining, the axial force on the inner lining increases, and the axial force on the outer lining decreases. And the magnitude of variance gradually weakens. When the thickness of the inner lining is about 47 cm, the axial force on the outer lining is zero. Although increasing the thickness of the inner lining can effectively reduce the axial force on the outer lining, the axial force of the inner lining will continue to increase on a larger basis. Therefore, the thickness of the inner lining should not be

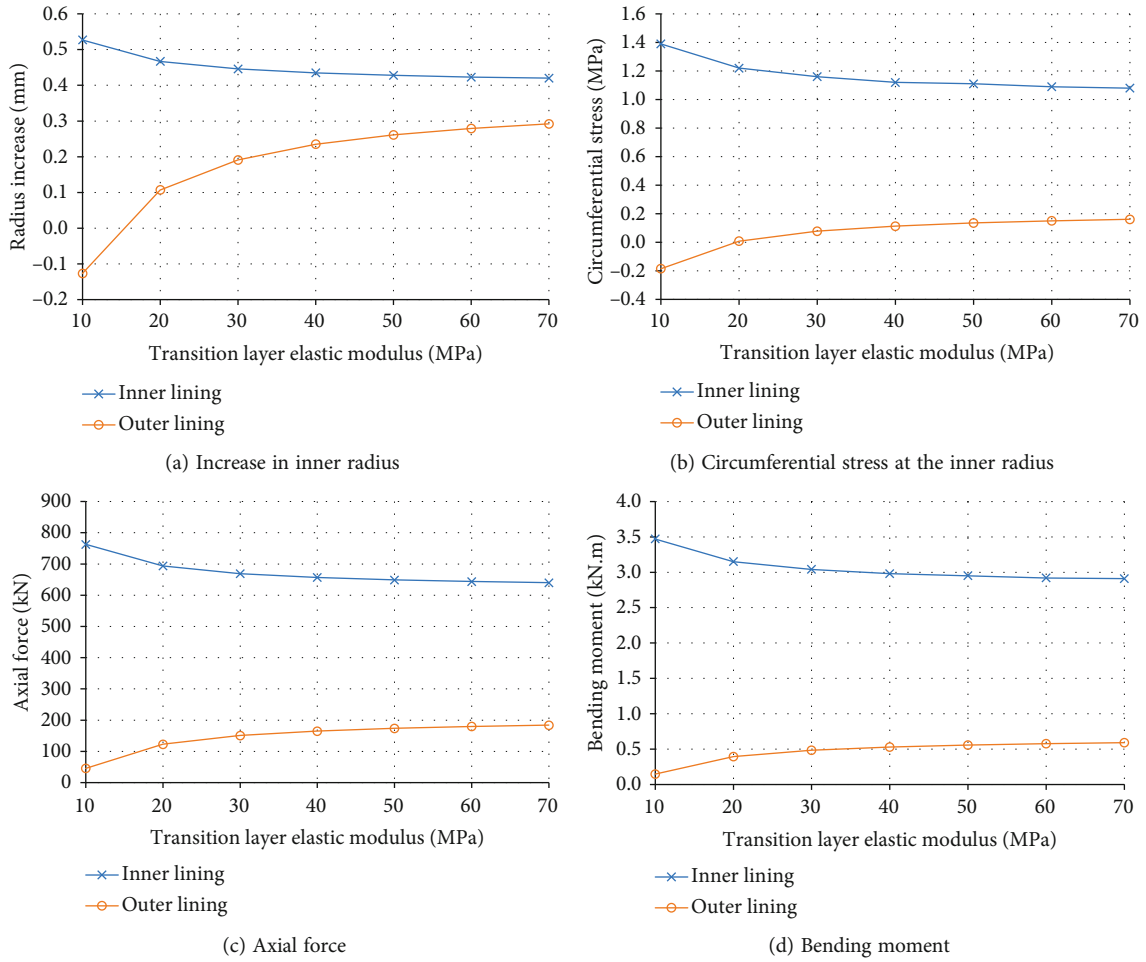

Figure 12: Influence of transition layer material on internal force and deformation of lining structure.

excessively increased in the design of the lining structure, and a better value should be taken under the balance of internal force and deformation.

It can be seen from Figure 11(d) that when the thickness of the inner lining is 20 cm, the bending moments on the inner and outer linings are almost equal and very small. With the increase of the thickness of the inner lining, the bending moment on the inner lining increases continuously, and the magnitude of variance gradually increases. The bending moment on the outer lining decreases continuously. When the thickness of the inner lining is about 47 cm, the bending moment on the outer lining is zero. The bending moment of the inner lining changes significantly with the increase of the thickness of the inner lining. Therefore, appropriately reducing the thickness of the inner lining can effectively reduce the bending moment generated on it.

4.2. Influence of Transition Layer Material on Internal Force and Deformation of Structure. Different materials filled in the transition layer between the inner lining and the outer lining will affect the deformation and stress of the whole structure to make the stress distribution and deformation control among structures more reasonable. According to the model parameters in Table 5, the influence of elastic modulus of transition layer material on the internal force and deformation of double-layer lining structure will be explored in the following.

The elastic modulus of transition materials is 1*e*4, 2*e*4, 3*e*4, 4*e*4, 5*e*4, 6*e*4, and 7*e*4 kPa, respectively. The lining structure bears 0.517 MPa internal uniform water pressure and 0.3 MPa external uniform water and soil pressure. According to the calculation method provided in this paper, the increment and circumferential stress at the inner radius of inner and outer linings as well as their respective axial forces and bending moments are calculated, as shown in Figure 12.

It can be seen from Figure 12(a) that with the increase of elastic modulus of transition layer material, the deformation of the inner radius of the inner lining decreases, and the deformation value of the outer lining increases. The magnitude of variance gradually weakens, and the difference of deformation between them is decreasing. When the elastic modulus of the transition layer is 15 MPa, the increase of the inner radius of the outer lining is almost zero. It shows that the phenomenon that the inner and outer linings bear the external pressure together is more obvious with increasing material thickness of the transition layer, and the radial deformation between them tends to be consistent gradually.

It can be seen from Figure 12(b) that with the increase of elastic modulus of the transition layer material, the circumferential stress at the inner radius of the inner lining decreases, and the circumferential stress at the inner radius of the outer lining increases. The change range of both is gradually slowing down. The circumferential stress at the inner radius of the inner lining is larger than that of the outer lining. Therefore, using materials with a larger elastic modulus under the condition of the constant thickness of the transition layer can reduce the circumferential stress generated by the inner and outer lining structures. At the same time, the inner lining should adopt an integral structure to avoid large gaps at the joints caused by excessive circumferential stress.

It can be seen from Figure 12(c) that with the increase of elastic modulus of the transition layer material, the axial force on the inner lining decreases, and the axial force on the outer lining increases. The change range of both is gradually slowing down. The axial force of the inner lining is much larger than that of the outer lining, and the axial force values of the inner and outer linings will obviously change with the variance of elastic modulus of the transition layer material. Therefore, adopting harder materials with a constant thickness of the transition layer can effectively reduce the maximum axial force values generated in the lining structure.

It can be seen from Figure 12(d) that with the increase of elastic modulus of the transition layer material, the bending moment of the inner lining decreases, and the bending moment of the outer lining increases. The change range of both is gradually slowing down. Its variation law is the same as that of inner radius deformation, circumferential stress, and axial force of inner and outer linings. They all show that the larger the elastic modulus of transition layer material is, the more obvious the phenomenon that both inside and outside bear the external pressure. And the larger the elastic modulus of the transition layer, the smaller the maximum deformation and internal force in the structure.

5. Conclusions

Based on the stress model of the water conveyance tunnel structure, this paper proposes a method to calculate the internal force and deformation of the double-layer lining structure. Compared with the results of numerical calculation and analytical solution, the correctness of the calculation method is verified. Finally, the factors affecting the internal force and deformation of the lining structure are further analyzed by the analytical method. Through the above analysis, the following conclusions are drawn:

(1) Based on the theory of elasticity, the deformation coordination relationship among structures is considered. In this paper, a simplified stress analysis model of composite double-layer lining is presented, and a series of parameters are derived. It can effectively calculate the displacement and internal force of this kind of lining structure

(2) The smaller the thickness of the transition layer or the harder the material, the more obvious the effect that the inner and outer linings of the composite double-layer lining structure bear the internal water pressure and external water and soil load together. At this time, the maximum deformation value and the maximum internal force value of the structure are smaller

(3) With the increase of inner lining thickness, the radial displacement and circumferential stress at the inner radius of the inner lining are greatly reduced. However, the internal force will increase, and the phenomenon that the inner and outer linings bear the internal and external pressure alone will be more obvious

The calculation method of internal force and deformation given in this paper analyzes the stress of each structure separately, considering the radial compression deformation of lining material, which is more in line with the actual situation. Because the resistance generated by surrounding rock and soil bodies is not considered, it is more suitable for the soil stratum. With more and more application scenarios of water conveyance tunnels and double-layer linings, the lateral and longitudinal mechanical analysis of the structure needs further study. In addition, the complex geological conditions, earthquake and structural damage, and other factors need to be deeply analyzed.

Data Availability

The data used to support the findings of this study are included in the article.

Conflicts of Interest

There is no conflict of interest in this study.

Acknowledgments

This work was supported by the National Natural Science Foundation of China (Grant No. 51508278).

References

[1] S. Wang, L. Ruan, X. Shen, and W. Dong, "Investigation of the mechanical properties of double lining structure of shield tunnel with different joint surface," *Tunnelling and Underground Space Technology*, vol. 90, pp. 404–419, 2019.

[2] K. Feng, C. He, Y. Fang, and Y. Jiang, "Study on the mechanical behavior of lining structure for underwater shield tunnel of high-speed railway," *Advances in Structural Engineering*, vol. 16, no. 8, pp. 1381–1399, 2013.

[3] C. Scalise and K. Fitzpatrick, "Chicago deep tunnel design and construction," *In Structures Congress*, vol. 2012, no. 2, pp. 1485–1495, 2012.

[4] R. Guo, M. Zhang, H. Xie, C. He, Y. Fang, and S. Wang, "Model test study of the mechanical characteristics of the lining structure for an urban deep drainage shield tunnel," *Tunnelling and Underground Space Technology*, vol. 91, article 103014, 2019.

[5] F. Yang, S. R. Cao, and G. Qin, "Mechanical behavior of two kinds of prestressed composite linings: a case study of the Yellow River crossing tunnel in China," *Tunnelling and Underground Space Technology*, vol. 79, pp. 96–109, 2018.

[6] T. D. Y. F. Simanjuntak, M. Marence, A. E. Mynett, and A. J. Schleiss, "Pressure tunnels in non-uniform in situ stress conditions," *Tunnelling and Underground Space Technology*, vol. 42, pp. 227–236, 2014.

[7] F. Yang, H. Zhou, C. Zhang, J. Lu, X. Lu, and Y. Geng, "An analysis method for evaluating the safety of pressure water conveyance tunnel in argillaceous sandstone under water-weakening conditions," *Tunnelling and Underground Space Technology*, vol. 97, article 103264, 2020.

[8] F. Yang, S. Cao, and G. Qin, "Performance of the prestressed composite lining of a tunnel: case study of the yellow river crossing tunnel," *International Journal of Civil Engineering*, vol. 16, no. 2, pp. 229–241, 2018.

[9] Y. Chen, Y. Wang, and Q. Y. Zhang, "Coupled seepage-elastoplastic-damage analysis of saturated porous media and its application to water conveyance tunnel," *Tunnelling and underground space technology*, vol. 44, pp. 80–87, 2014.

[10] G. H. Yang, Z. Y. Li, C. B. Xu, K. Jia, and Y. Jiang, "Load-structure interaction model of shield tunnel composite lining," *Journal of Hydroelectric Engineering*, vol. 37, no. 10, pp. 20–30, 2018.

[11] M. Ghorbani, K. Shahriar, M. Sharifzadeh, and R. Masoudi, "A critical review on the developments of rock support systems in high stress ground conditions," *International Journal of Mining Science and Technology*, vol. 30, no. 5, pp. 555–572, 2020.

[12] R. Shakeri, A. Mesgouez, and G. Lefeuve-Mesgouez, "Transient response of a concrete tunnel in an elastic rock with imperfect contact," *International Journal of Mining Science and Technology*, vol. 30, no. 5, pp. 605–612, 2020.

[13] H. Rehman, A. M. Naji, W. Ali, M. Junaid, R. A. Abdullah, and H. K. Yoo, "Numerical evaluation of new Austrian tunneling method excavation sequences: a case study," *International Journal of Mining Science and Technology*, vol. 30, no. 3, pp. 381–386, 2020.

[14] A. Haghighat and K. Luxbacher, "Determination of critical parameters in the analysis of road tunnel fires," *International Journal of Mining Science and Technology*, vol. 29, no. 2, pp. 187–198, 2019.

[15] H. Farhadian, "A new empirical chart for rockburst analysis in tunnelling: tunnel rockburst classification (TRC)," *International Journal of Mining Science and Technology*, vol. 31, no. 4, pp. 603–610, 2021.

[16] Y. Jin, W. Ding, Z. Yan, K. Soga, and Z. Li, "Experimental investigation of the nonlinear behavior of segmental joints in a water-conveyance tunnel," *Tunnelling and Underground Space Technology*, vol. 68, pp. 153–166, 2017.

[17] D. Pan, K. Hong, H. Fu et al., "Numerical simulation of nano-silica sol grouting for deep tunnels based on the multifield coupling mechanism," *Geofluids*, vol. 2021, Article ID 3963291, 14 pages, 2021.

[18] J. Z. Zhang, H. W. Huang, D. M. Zhang, M. L. Zhou, C. Tang, and D. J. Liu, "Effect of ground surface surcharge on deformational performance of tunnel in spatially variable soil," *Computers and Geotechnics*, vol. 136, article 104229, 2021.

[19] T. Deng, S. Norris, and R. N. Sharma, "Numerical investigation on the stability of tunnel smoke stratification under the effect of water spray and longitudinal ventilation," *Tunnelling and Underground Space Technology*, vol. 112, article 103901, 2021.

[20] Z. Yan, K. Liu, and Y. Shen, "Numerical study on mechanical properties of large diameter double-layer shield tunnels under the elevated temperatures in fire," *IOP Conference Series: Earth and Environmental Science*, vol. 861, no. 7, article 072045, 2021.

[21] Q. J. Chen, J. C. Wang, W. M. Huang, Z. X. Yang, and R. Q. Xu, "Analytical solution for a jointed shield tunnel lining reinforced by secondary linings," *International Journal of Mechanical Sciences*, vol. 185, article 105813, 2020.

[22] E. H. Naggar, S. D. Hinchberger, and M. H. E. Naggar, "Simplified analysis of seismic in-plane stresses in composite and jointed tunnel linings," *Soil Dynamics and Earthquake Engineering*, vol. 28, no. 12, pp. 1063–1077, 2008.

[23] D. P. Do, M. N. Vu, N. T. Tran, and G. Armand, "Closed-form solution and reliability analysis of deep tunnel supported by a concrete liner and a covered compressible layer within the viscoelastic burger rock," *Rock Mechanics and Rock Engineering*, vol. 54, no. 5, pp. 2311–2334, 2021.

[24] H. Murakami and A. Koizumi, "Behavior of shield segment ring reinforced by secondary lining," *Doboku Gakkai Ronbunshu*, vol. 1987, no. 388, pp. 85–94, 1987.

[25] S. Li, Y. G. Zhang, M. Y. Cao, and Z. N. Wang, "Study on excavation sequence of pilot tunnels for a rectangular tunnel using numerical simulation and field monitoring method," *Rock Mechanics and Rock Engineering*, vol. 18, no. 7, pp. 1–17, 2022.

[26] H. Wu, G. Y. Zhao, and S. W. Ma, "Failure behavior of horseshoe-shaped tunnel in hard rock under high stress: phenomenon and mechanisms," *Transactions of Nonferrous Metals Society of China*, vol. 32, no. 2, pp. 639–656, 2022.

[27] M. M. He, Z. Q. Zhang, J. W. Zhu, and N. Li, "Correlation between the constant mi of hoek-brown criterion and porosity of intact rock," *Rock Mechanics and Rock Engineering*, vol. 55, no. 2, pp. 923–936, 2022.

[28] B. Yang, M. He, Z. Zhang, J. Zhu, and Y. Chen, "A new criterion of strain rockburst in consideration of the plastic zone of tunnel surrounding rock," *Rock Mechanics and Rock Engineering*, vol. 55, no. 3, pp. 1777–1789, 2022.

[29] J. Ma, X. L. Li, J. G. Wang et al., "Experimental study on vibration reduction technology of hole-by-hole presplitting blasting," *Geofluids*, vol. 2021, 10 pages, 2021.

[30] J. Wang, T. Zuo, X. Li, Z. Tao, and J. Ma, "Study on the fractal characteristics of the pomegranate biotite schist under impact loading," *Geofluids*, vol. 2021, Article ID 1570160, 2021.

[31] D. Pan, K. Hong, H. Fu, J. Zhou, and N. Zhang, "Experimental study of the mechanism of grouting colloidal nano-silica in over-broken coal mass," *Quarterly Journal of Engineering Geology and Hydrogeology*, vol. 54, no. 4, 2021.

[32] Y. G. Zhang, J. Tang, Y. M. Cheng et al., "Prediction of landslide displacement with dynamic features using intelligent approaches," *International Journal of Mining Science and Technology*, vol. 2, no. 1, pp. 1–11, 2022.

[33] D. Pan, K. Hong, H. Fu, J. Zhou, N. Zhang, and G. Lu, "Influence characteristics and mechanism of fragmental size of broken coal mass on the injection regularity of silica sol grouting," *Construction and Building Materials*, vol. 269, article 121251, 2021.

[34] G. S. Han, Y. Zhou, R. Liu, Q. Tang, X. Wang, and L. Song, "Influence of surface roughness on shear behaviors of rock joints under constant normal load and stiffness boundary conditions," *Natural Hazards*, vol. 2, pp. 1–19, 2022.

[35] F. Li, N. Chang, J. Wang, T. Feng, and C. Li, "Research on the algorithm for composite lining of deep buried water conveyance tunnel," *Advances in Civil Engineering*, vol. 2021, no. 12, 2021.